Prepared for the
National Institutes of Health
National Institute of Neurological Disorders and Stroke
Neural Prosthesis Program
Bethesda, MD 20892

ELECTRODES FOR FUNCTIONAL NEUROMUSCULAR STIMULATION

Contract #NO1-NS-32300

Quarterly Progress Report #2
1 December, 1993 - 28 February, 1994

Principal Investigator
J. Thomas Mortimer, Ph.D.

Co-Investigator
Warren M. Grill, M.S.

Applied Neural Control Laboratory
Department of Biomedical Engineering
Case Western Reserve University
Cleveland, OH 44106

Table of Contents

Section B: Electrode Design and Fabrication

B.1.b Multiple Contact Spiral Nerve Cuff Electrodes

During this quarter we have fabricated silicone rubber spiral nerve cuff electrodes containing twelve individually addressable platinum electrode contacts. Electrodes were fabricated using two different methods as described below.

The first series of electrodes were fabricated for use in acute animal experiments. Spiral nerve cuffs were fabricated by modifying the method of Naples *et al.* [1988] to create a tri-layer silicone rubber cuff that included 4 longitudinal tripoles of recessed 1 mm diameter platinum dot electrodes, each with a separate lead. The design allows implementation of a tripolar electrode configuration (cathode between two anodes) at four locations every 90° around the circumference of the nerve trunk, and use of transverse field steering current from a dot electrode located 180° around the trunk from the cathode of the tripole.

Three rows of four perforations each were made in a 50 µm thick sheet of silicone rubber (SCIMED Surgical, Minneapolis, MN) using a 23-gauge hypodermic needle. The rows were spaced 5 mm apart and the distance between perforations in each row was between 2.0 and 2.75 mm, depending on the intended final inside diameter of the cuff (2.5 to 3.5 mm). Teflon® insulated multistrand 316L stainless steel wires (1x7x35µm, Cooner Wire Co., Chatsworth, CA) were spot-welded to 2 mm by 1 mm pieces of 35 µm thick platinum foil (Johnson Mathey, Pittsburgh, PA) and were passed through each perforation until all the electrodes lay flat on the silicone rubber sheet. The position of each electrode in the array was thus determined by the position of the perforation. The middle sheet, with the platinum electrodes facing downward, was clamped at both ends, stretched, and bonded to a second 50 µm thick unstretched sheet of silicone rubber as described by Naples, *et al.* [1988]. The lead wires ran between the two sheets and were oriented perpendicularly to the direction of stretch. A third 50 µm thick silicone rubber sheet was clamped at both ends, stretched, and bonded to the bilayer of the outer and middle sheets containing the electrodes. Circular windows, 1 mm in diameter, were cut in the inner layer using a sharpened section of hypodermic tubing to expose the electrode surfaces, yielding electrode contacts that were recessed by 50µm below the inner surface of the cuff. The cuff, with the 12 leads, was cut out and trimmed to a width of 20 mm leaving 5 mm between each external row of electrode contacts and the ends of the cuff. The length of the unrolled cuff was trimmed to between 32 and 50 mm, depending on the diameter of the nerve trunk, in order to provide two full wraps of the cuff around the nerve trunk. The diameters of the cuffs were between 2.5 and 3.5 mm to fit the range of diameters measured for the cat sciatic nerve [Veraart *et al.*, 1993].

The fabrication methods described above were modified to produce a second series of electrodes intended for chronic implantation. In these electrodes all twelve leads were routed out one end of the cuff, rather than six leads exiting from each

end. The spacing between the electrodes in a row (i.e., the longitudinal distance between the anodes and the cathode in each tripole) was reduced from 5 mm to 3mm. Our simulation results indicated that closer spacing between the anodes and cathode should improve spatial selectivity [Chintilacharuvu et al., 1994], and the change in inter electrode spacing allowed the overall length of the cuff to be reduced by 40%, from 2 cm to 1.2 cm. The diameter of the window cut in the inner sheet of silicone rubber was also reduced from 1.0 mm to 0.5 mm in a effort to improve selectivity.

The twelve lead wires were formed into a single lead cable to facilitate subcutaneous passing and percutaneous exit. The wires were grouped together and passed through 3 mm sections of silicone rubber tubing (Dow Corning Silastic 602-205, 1.0 mm I.D., 2.2 mm O.D.) every 6 cm. The sections of tubing were glued to the lead wires using silicone rubber elastomer (Dow Corning MDX 4-4210). At the exit end of the lead cable, the 12 leads were divided into 4 groups of 3 (one group for each tripole) and passed through smaller sections of silicone rubber tubing (Dow Corning Silastic 602-155, 0.6 mm I.D., 1.2 mm O.D.). The length of the small sections of tubing was used to code which leads belonged to each of the four tripoles (i.e., 1 mm section of tubing corresponded to tripole 0°, 2 mm section of tubing corresponded to tripole 90°, and so on).

B.1.c Fabrication of Helical Spiral Cuff Electrodes

The Helical-Spiral Cuff Electrode is intended to provide selective stimulation of peripheral nerves with the added benefits of endoscopic implantation. This electrode cuff takes advantage of the self-sizing characteristics of the spiral cuff to form intimate contact with the nerve without causing damage. In order to fit into endoscopic surgical implant tools, the cuff must be much narrower than the traditional spiral cuff. To accomplish this, the grid like pattern of the spiral cuff has been modified to a linear pattern for the helical-spiral cuff (Figure 1).

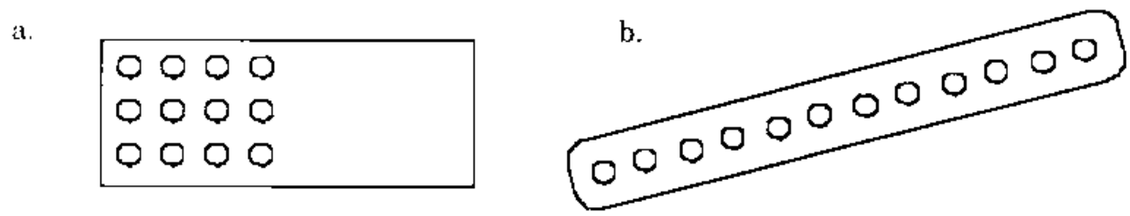

Figure 1: The planar layout pattern of: a. The traditional spiral cuff and b. The new helical-spiral cuff.

The helical-spiral cuff wraps around the nerve in such a way that each wrap has its respective electrodes line up with the electrodes of the previous wrap to form tripoles, as in Figure 2.

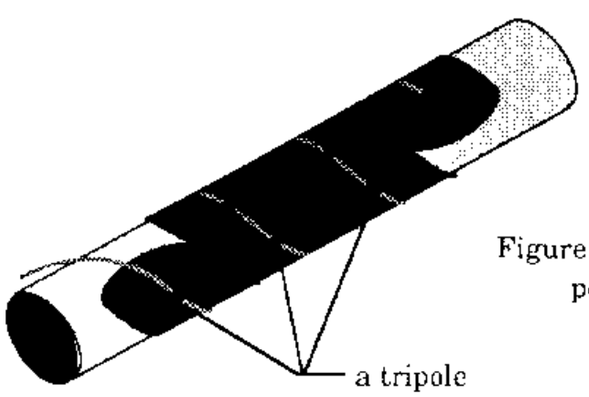

Figure 2: The helical-spiral cuff shown positioned around a nerve.

The basic production process is similar to the spiral cuff in that the cuff is made in a planar fashion, using sheets of silastic bonded together at different lengths to cause a curling tendency. The helical spiral has two main dimensions of concern for the production process: stretch percentage, the percent of resting length that the elastic sheet must be stretched, and the angle at which the cuff needs to be oriented with respect to the direction of stretch. The parameters then used to find these

quantities are D, the diameter of the cuff and G, the distance the midpoint of the cuff moves laterally over the course of one wrap around the nerve. A variation of an equation from Naples to approximately relate the stretch to the diameter, D is:

$$\% \text{ Stretch} = 2 * T / D$$

where T is the average thickness of the cuff. This equation, which defines the stretch for a given T, is based on a cuff made of purely elastic material. The effects of the spine of the cuff as well as the metal wires inside the cuff, must be taken into account. Due to primarily the metal wires, steps had to be taken to maximize the curling effect. One change was to use 25um monofilament wire instead of the 7 stranded 125um wire. In addition to the change in wire, the unstretched thickness of the cuff was minimized. It is important to reduce the unstretched thickness, as opposed to the total thickness, since the above equation assumes that both sides of the cuff will return to their resting lengths, which will not occur when the metal and the spine are added to the cuff. To minimize this thickness, the unstretched sheet of silicone used in fabricating the spiral cuff electrode was eliminated. The helical spiral is therefore fabricated using one stretched sheet over the electrodes and elastomer, without the additional unstretched sheet underneath. Using both of these modifications, we are able to get the diameter of the cuffs to be approximately 3mm with %stretch values around 80%.

The equation for the angle of the cuff with respect to the direction of stretch is:

$$\text{Angle} = \text{Tan}^{-1}(G/\pi D)$$

where D is the final diameter of the cuff, and G is the distance from midpoint to midpoint of successive wraps of the cuff. The angle calculated is then used to orient the coiled wires with the electrode contacts with respect to the stretched sheet during construction.

Once the elastomer has cured, the windows over the contacts are cut and each contact is tested to verify that each electrode is still contiguous. The final step in production is to cut out the helical-spiral and trim the edges.

B.1.d Thin Film Fabrication Techniques

i.) Electrode Fabrication

In the original proposal we specified that we would purchase thin film electrode substrates from Patrick van der Puije at the University of Ottawa. Unfortunately Dr. van der Puije has lost his technician and will be unable to fabricate electrodes until at least June, 1994. Therefore, we have elected to obtain thin film electrodes from Dr. Stuart Cogan at EIC Laboratories. Dr. Cogan has developed techniques, under NIH SBIR support, to deposit and pattern metallization (titanium/platinum and titanium/iridium) on Teflon substrates.

We have designed a mask pattern that includes 12-electrode spiral cuffs and 12-electrode helical spiral cuffs. Figure 3 illustrates the layout of electrode contacts and thin-film leads for each of the two designs. We are having masks fabricated at the Electronics Design Center here at Case Western Reserve University. After the masks are completed we will send them to Dr. Cogan who will provide us with metallized, patterned, and insulated substrates. We expect to begin testing of completed thin film electrodes by the end of the third quarter.

ii.) Methods to Attach Lead Wires to Thin Films

We are conducting a study to evaluate the strength and electrical properties of conductive epoxy (see Quarterly Progress Report #1). We have completed testing of control samples and are presently evaluating samples that were soaked in elevated temperature saline to accelerate degradation. The results of this study will be reported in QPR #3.

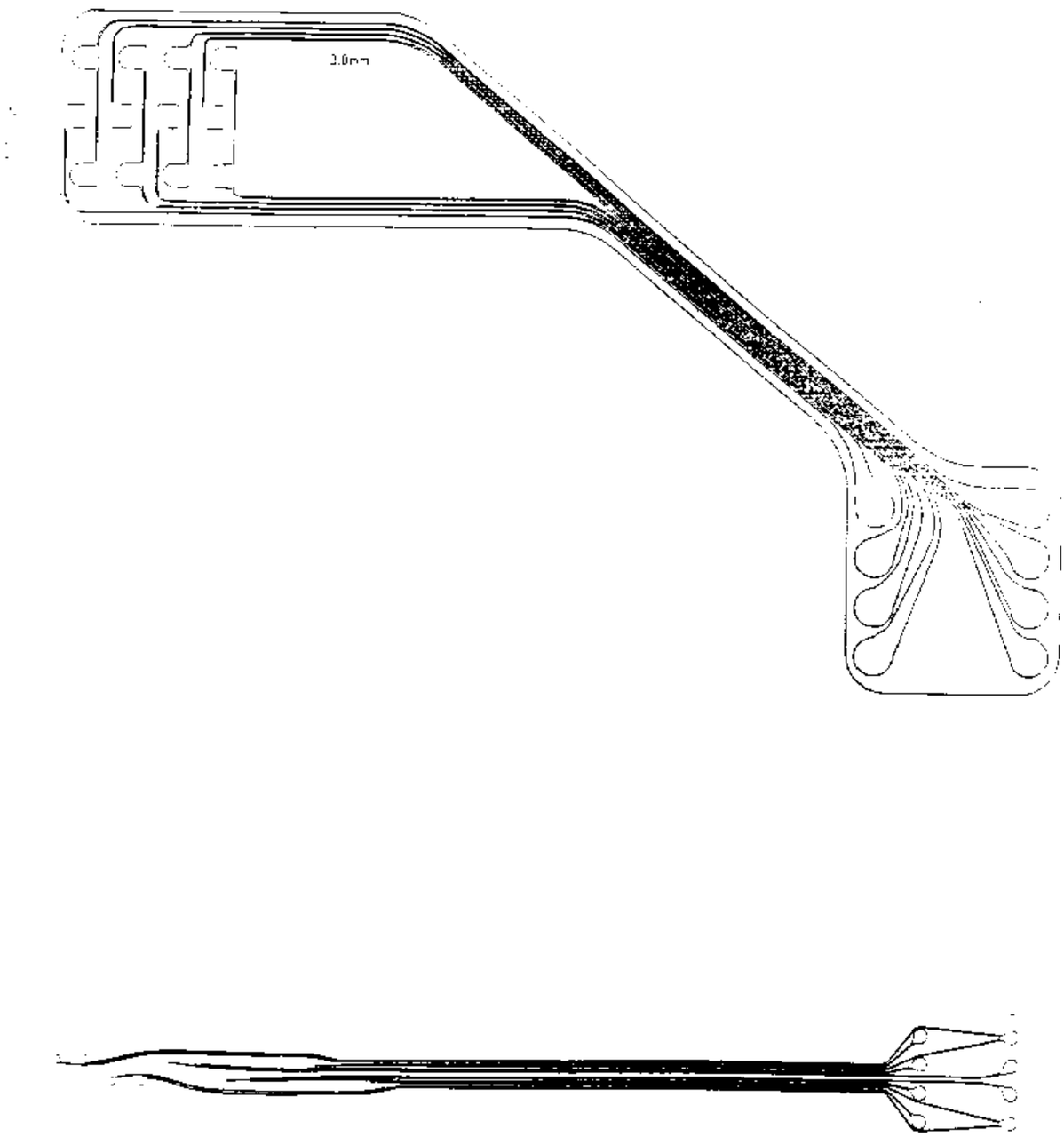

Figure 3: Layout of electrode contacts and thin-film leads for fabrication of thin film electrodes. In both designs, the anodes in each tripole are connected to a common lead to reduce the number of leads from 12 to 8. top)- Layout for 12-electrode spiral nerve cuff. bottom) Layout for 12-electrode helical spiral nerve cuff.

Section C: Assessment of Electrode Performance in an Animal Model

Design and Fabrication of a General Purpose, Computer Controlled, Laboratory Stimulator

A new nerve stimulator capable of improving the efficiency of experiments has been developed. The stimulator (LABSTIM) was specifically designed to be controlled by a personal computer. A sequence of coded pulses, transmitted via two input/output digital lines, determine all stimulation parameters. Pulse width, frequency, and amplitude of stimulation can be preset by the computer. Pulse parameters can also be updated during stimulation, which allows the generation of a burst of stimuli with gradually changing pulse widths, frequencies, or amplitudes. Pulse width range is 10 usec - 10 msec, and the range of frequency is 0.1 Hz - 1 KHz. The maximum amplitude that can be generated by the stimulator is 25 mA.

The output stimulus is a regulated current pulse which can be monophasic or biphasic. In the case of biphasic stimulation the charge of the cathodic phase is equal to that of the anodic phase (charge balanced). Current during the anodic phase is controlled and internally set to 200 uA. Monophasic and biphasic waveforms can be selected by the computer.

LABSTIM has the ability to generate a slowly decaying transition at the end of the cathodic phase of the current pulse (Quasi-trapezoidal pulses). The time constant of this decay is determined by the computer and can vary from 0 usec (no decay) to 700 usec. This option can be used in experiments where nerve excitation can be produced by a sudden transition at the end of the cathodic phase (i.e., anodic break).

LABSTIM offers outputs for a tripolar electrode configuration (anode, cathode, anode). Bipolar electrode configuration can be attained by using the cathode and one of the anodes. In the case of tripolar configuration, the current flowing through each anode is the same (their sum is equal to the current flowing through the cathode). However, the stimulator allows the ability to decrease the current flowing in one of the anodes and increase it in the other keeping their sum equal to the cathodic current. This current imbalance is adjusted manually and is not controlled by the computer.

The stimulator derives its power from a single 9V battery, which should maintain the stimulator for approximately 60 hours under continuous operation. Battery life is continuously monitored and an indicator lights if a low battery voltage is detected.

The hardware described above is for a single channel stimulator (one tripolar electrode output). Multiple channels can be generated by duplicating the hardware. A four channel stimulator is currently available.

This system is presently interfaced with a Macintosh IIfx. A menu driven software interface has been developed to provide the required communication protocol for transmission of parameter values to the stimulator. This program uses the Labview software package and two computer boards (I/O and timer boards) all manufactured by National Instruments. The program has been expanded to include data acquisition and analysis as well. Hence, the same program can now control stimulation as well as data collection simultaneously. The present program can handle communications for an eight channel stimulator.

C.1.a Performance Testing in Acute Animal Experiments
C.1.c Quantitative Analysis of Electrode Performance

During this quarter, we have conducted 10 acute experiments on adult cats to quantify the recruitment properties of the 12 contact spiral cuff electrode. Appendix I contains a manuscript (submitted to the Journal of Neuroscience Methods) that describes in detail the methods we have used to measure the recruitment properties. During the next quarter we will complete analysis of the data from the acute experiments and prepare a manuscript reporting on the input-output properties of the cuff electrode.

REFERENCES

Chintilacharuvu, R.R., D.A. Ksienski, and J.T. Mortimer (1994) A numerical analysis of the electric field generated by a nerve cuff electrode using the finite element method. IEEE Trans. Biomed. Eng., in press.

Naples, G. G., J. T. Mortimer, A. Scheiner, and J.D. Sweeney (1988)A spiral nerve cuff electrode for peripheral nerve stimulation. IEEE Trans. Biomed. Eng. 35: 905-916.

Veraart C., W.M. Grill, and J.T. Mortimer (1993) Selective control of muscle activation with a multipolar nerve cuff electrode. IEEE Trans. Biomed. Engineering 40(7):640-653.

Appendix I

Non-Invasive Measurement of Recruitment Properties of Implanted Electrodes

Warren M. Grill and J. Thomas Mortimer

submitted to J. of Neuroscience Methods

ABSTRACT

Recruitment properties describe the input-output characteristics of neural stimulating electrodes. A non-invasive method was developed to measure the recruitment properties of electrodes activating peripheral motor neurons. A custom apparatus was designed to measure the three-dimensional isometric torque generated at the ankle joint by electrical activation of the cat sciatic nerve. The performance of the apparatus was quantified, and the utility of the method was demonstrated by measuring the recruitment properties of a multiple contact nerve cuff electrode. It was found that the peak of the twitch torque was an accurate measure of excitation, and that the shape of the torque waveform provided information about the relative diameters of the nerve fibers that were activated. The contributions of rapidly and slowly contracting muscle fibers to the ankle joint torque were determined. The magnitudes and directions of the torques produced by activation of individual fascicles of the sciatic nerve were also determined. The methods described are useful for characterization of neural stimulating electrodes and for studies of motor system physiology.

Key Words: recruitment, electrodes, joint torque, motor prostheses, neural stimulation, cat, ankle joint, sciatic nerve

INTRODUCTION

Electrical activation of intact lower motor neurons can restore movement to spinal cord injured persons [Stein et al., 1992]. Present motor system neural prostheses employ either coiled wire intramuscular electrodes [Memberg et al., 1993] or epimysial disk electrodes [Grandjean and Mortimer, 1986] to excite motor neurons. These muscle-based electrodes have been used to restore hand grasp to quadriplegics [Gorman and Peckham, 1991], and standing and stepping in paraplegics [Marsolais and Kobetic, 1987]. It is anticipated that future systems will require more channels of stimulation for greater function. For more complex systems, nerve electrodes offer several advantages over muscle based electrodes [Naples et al., 1990]. Nerve electrodes can also be applied where muscle size or anatomy precludes the use of muscle electrodes [Mortimer and Grill, 1993]. A number of different nerve electrodes are under development including cuff electrodes placed around the nerve trunk [McNeal and Bowman, 1985, Veraart et al., 1993], wire electrodes sutured to the epineurium [Thoma et al., 1987], and intrafascicular electrodes placed within the endoneurium [Bowman and Erickson, 1985, Veltink et al., 1985, Nannini and Horch, 1991, Rutten et al., 1991]. Before an electrode can be considered for application in humans, its safety and efficacy must be firmly established. Efficacy is assessed by measuring input-output properties of the electrode-motor nerve-muscle system. These properties are generally referred to as recruitment properties, and are loosely defined as the motor output generated per unit of stimulus input (e.g., stimulus amplitude, stimulus duration or stimulus frequency).

Recruitment properties have most commonly been evaluated by measuring the force generated in isolated whole muscle(s) by different electrical stimuli. These studies have yielded important insights about the recruitment characteristics of intramuscular electrodes [Crago et al., 1980], epimysial electrodes [Grandjean and Mortimer, 1986], nerve cuff electrodes [Gorman and Mortimer, 1983, McNeal et al., 1989, Veraart et al., 1993], and intraneural electrodes [Veltink et al., 1985, Nannini and Horch, 1991, Rutten

et al., 1991]. This method, however, is not suitable for serial chronic testing of electrode recruitment properties because it requires tenotomy to measure muscle force. An alternative method to measure individual muscle force is to use implanted tendon force buckle transducers [Hoffer, 1990]. However, this method is limited by inaccuracies due to friction, viscoelasticity, chronic tissue adaptation, and difficulty in defining zero force [Ashton-Miller et al., 1992]. Both these methods are also limited in the number of muscles that can simultaneously be recorded.

It is also important to quantify the effect of joint angle changes on recruitment properties. Angle-dependent recruitment makes control of electrically activated muscle difficult, creates regions of high and variable gain, and may limit range of motion by causing instabilities. Angle dependence arises from the intrinsic length-tension properties of muscle [Rack and Westbury, 1969], from angle dependent moment arms [Young et al., 1992], and from changes in the geometrical relationship between the stimulus field and the excitable fibers due to relative movement between the electrode and the motor nerve fibers (i.e., angle-dependent recruitment). The effect of muscle length on recruitment properties has been examined for intramuscular and epimysial electrodes [Crago et al., 1980, Grandjean and Mortimer, 1983], however, because muscle moment arms depend on joint angle [Young et al., 1992], and altering joint angle simulates the motion that will occur in motor prosthetic applications, joint angle dependence of recruitment properties is a more appropriate measure of positional stability.

The first goal of this work was to develop a non-invasive method to measure the recruitment properties of implanted stimulating electrodes. A method was needed to make repeated measurements of recruitment properties over time, and to determine the angle-dependence of electrode recruitment properties. The second goal of this work was to determine an appropriate measure of the level of muscle activation based on the muscle twitch response. Twitch contractions are widely employed in testing of

recruitment properties to minimize the effects of muscle fatigue. The peak of the twitch response has been used as a measure of the activation level of a muscle. Such a measure, however, does not take into account the different contraction speeds of the individual motor units. Therefore, the peak of the twitch may underestimate the level of activation of slowly contracting muscle fibers. To determine an appropriate measure of muscle activation, the level of activation predicted by the peak of the twitch was compared to the level of activation predicted by the area under the twitch.

METHODS

Experimental Apparatus

A system was designed and fabricated to measure the three-dimensional isometric torque generated at the cat ankle joint by electrical stimulation of the sciatic nerve. The system was built around a commercially available three-dimensional force transducer (JR^3, Woodland, CA, Model UFS-3A25-U560) that employs foil strain gauges to measure forces in six degrees-of-freedom (force acting in the x, y, and z directions and moments about the x, y, and z axes). The sensor electronics provide analog outputs of digitally de-coupled signals, yielding measures of the different components of force and moment virtually free of cross-talk (see below).

The force sensor was included in a custom apparatus to interface with the cat hindlimb (figure 1). The force sensor was mounted on a 1/2" thick stainless steel faceplate which was able to slide along two rods. This allowed adjustment of the anterior-posterior position of the ankle joint. The rods were fixed at one end in Kopf micropositioner carriers and at the other end were supported in sliding blocks on a rigid frame. This allowed the ankle joint angle to be varied in the sagittal plane (plantar-flexion/dorsi-flexion direction). The Kopf micropositioner carriers were mounted on a custom support that was also mounted in sliding blocks on the rigid frame. This allowed positioning of the ankle joint relative to the knee. The foot was mounted

perpendicular to the sensor face using a custom built aluminum shoe. The shoe was adjustable in the dorsal-plantar direction to align the center of the sensor with the inversion-eversion axis of the ankle joint. The foot was held in the shoe using a tongue made of thermofit casting material and 3 plastic tie wraps. The knee was held fixed using a pair of cup clamps over the distal head of the femur, and the hip was clamped in place to prevent trunk displacements generated by large plantar-flexion torques at the ankle.

Experimental Procedure

Acute experiments were conducted on three adult cats. All animal care and procedures were according to NIH guidelines and were approved by the Institutional Animal Care and Use Committee of Case Western Reserve University. Animals were initially anesthetized with ketamine hydrochloride (35 mg/kg, I.M.), and atropine sulfate (0.05 mg/kg, I.M.) was administered to reduce salivation. Animals were intubated, a catheter was inserted in the cephalic vein, and a surgical level of anesthesia was maintained with sodium pentobarbital (5-10 mg bolus injections, I.V.). A silicone rubber cuff electrode containing 12 individually addressable platinum contacts [Veraart et al., 1993] was implanted on the right sciatic nerve 1-2 cm proximal to the bifurcation into tibial and common peroneal components.

The animal was mounted in the measurement apparatus as shown in figure 1 with the ankle, knee, and hip joint angles set to 90±5°, 100±10°, and 110±10° degrees, respectively. The sensor was set-up to measure plantar-flexion/dorsi-flexion forces, toe-in/toe-out forces, and inversion/eversion torques (figure 2). Ankle joint torques were calculated by multiplying the forces by the moment arm (15.1±0.2 cm, mean±standard deviation, n=3) measured from the rotation center of the ankle joint to the center of the sensor with a resolution of ±0.1 cm.

Stimulation and Recording

Isometric twitch contractions were generated in the ankle musculature by selective electrical stimulation of the sciatic nerve via the implanted cuff electrode [Veraart et al., 1993]. The torque responses generated by stimulation of individual branches of the sciatic nerve (tibial, common peroneal, medial gastrocnemius, and lateral gastrocnemius/soleus) with a bipolar hook electrode were also recorded. In one experiment EMGs were recorded from soleus, medial gastrocnemius, and lateral gastrocnemius using bipolar intramuscular wire electrodes.

The stimuli were monophasic or biphasic 10us rectangular regulated current pulses delivered at 0.5 Hz from a stimulator designed and built in our laboratory. Stimulus amplitude was set manually with calibrated potentiometers. Five twitch responses were collected at each stimulus amplitude. The torque signals were low pass filtered at 100 Hz and sampled at 200 Hz with a 12-bit A/D converter. EMG signals were bandpass filtered (10 Hz-1 kHz), amplified, and sampled at 2 kHz.

The data collection system was based on a multiple function input-output board (NB-MIO-16H, National Instruments, Austin TX) and software written in LabVIEW (National Instruments, Austin, TX) running on a Macintosh Quadra 950. The software controlled stimulus pulsewidth, stimulus frequency, data sampling, and real time analysis and display. Twitch waveforms and EMGs for each set of stimulus parameters were averaged and saved. The peak torque and the torque-time integral (i.e., area under the torque twitch waveform) were calculated and saved. A real time display of the torque twitches, EMGs, and a recruitment curve of the peak torque as a function of the stimulus current amplitude was provided to the experimenter.

RESULTS

Qualification of the Measurement Apparatus

Known masses were applied to the aluminum shoe to simulate loading that would occur by generation of torques at the ankle joint. The coordinate system for measurement of ankle joint torques is shown in figure 2. The on-axis resolution was 0.054 N/bit for the **x** (toe-in/toe-out) and **y** (dorsi-flexion/plantar-flexion) axes, and was 0.415 N-cm/bit for the **z** (inversion/eversion) axis. The off-axis sensitivity (cross-talk) was less than 2% between the two force axes (**x** and **y**) and less than 3% between the two force axes and the moment axis (**z**). The repeatability was 0.06 N (i.e., standard deviation was 0.03 N, n=11) for a 1 kg mass applied repeatedly in one session. Similar repeatability was measured between two different sessions between which the apparatus had been taken apart and re-assembled. The response of the measurement system was linear between 0.5 N and 50 N (r^2=.989). Measurements of applied force were independent of the point of application of the force (<1% change in the output of the sensor for a 4 cm deviation in the point of application of the mass), and independent of the position of the apparatus (<1% change in the output of the sensor for ±25° displacements in the flexion-extension direction).

Recruitment Information in Torque Twitches

Application of single electrical stimuli to the sciatic nerve generated twitch contractions in the muscles of the shank that were measured as torques about the ankle joint. The twitch torque waveforms varied according to the electrode configuration and the amplitude of the stimulus (these variables determined the nerve fibers that were activated, see Veraart et al., 1993), as well as the speed and force of contraction of the muscle fibers innervated by the excited nerve fibers. Three types of recruitment information were obtained from the twitch waveforms: the amplitude of the torque

evoked by a particular stimulus, the direction of the resultant torque vector, and the relative diameters of the axons that were activated.

Examples of twitch waveforms obtained by both stimulation with the cuff electrode and supramaximal stimulation of individual nerve branches with a hook electrode are shown in figure 3. The individual fascicles innervating lateral gastrocnemius (LG) and soleus (SO), medial gastrocnemius (MG), and the common peroneal (CP) fascicle were selectively activated using different electrode combinations within the cuff [Veraart et al., 1993]. Note that the shape and amplitude of the twitch waveforms generated by activation with the cuff electrode were very similar to those obtained by stimulation of the individual nerve branches. At lower stimulus amplitudes (e.g., 200μA in fig. 3a) larger nerve fibers, which innervate more rapidly contracting muscle fibers, were activated and the twitch had a bell shape with a monotonically increasing rising phase and a monotonically decreasing falling phase. Additional nerve fibers were activated as the stimulus amplitude was increased, and the amplitude and duration of the primary twitch (P1) were increased. In some cases a second peak (P2) appeared. The second peak indicated activation of the smaller nerve fibers innervating slowly contracting muscle fibers. The latency of the first peak was 75 ± 5 ms, and the latency of the second peak was 150 ± 5 ms. In figure 3a, the second peak is very prominent and indicates that the nerve fibers innervating the SO muscle, which in the cat consists entirely of slow twitch muscle fibers [Burke et al., 1974], were being activated. This was verified by EMG recordings which indicated that appearance of the second peak was correlated with activation of the soleus muscle. Furthermore, when the soleus was tenotomized and reflected the amplitude of the second peak was greatly diminished. In all cases the slow component of the waveform was much larger when the fascicle innervating the LG and SO was stimulated than when the fascicle innervating the MG was stimulated. A smaller secondary peak from MG (figure 3b) is consistent with the smaller percentage of MG slow twitch muscle fibers as compared to

the SO [Burke et al., 1973]. The secondary peak was also smaller for activation of the common peroneal fascicle (figure 3c), consistent with the small population of slow twitch nerve fibers in the primary dorsiflexors of the ankle (tibialis anterior and extensor digitorum longus) [Dum and Kennedy, 1980].

The torques generated by the two fiber size populations (i.e., P1 and P2) in the plantar-flexion/dorsi-flexion direction are plotted in figure 4 as a function of the stimulus current for each of the three fascicles represented in figure 3. The curves in figure 4a illustrate the threshold difference between the large nerve fibers innervating LG and the small nerve fibers innervating SO. There was a large increase in P1 between 100 μA and 200 μA, but no increase in P2, because small nerve fibers innervating slowly contracting muscle fibers have a higher recruitment threshold for extracellular stimulation than do large nerve fibers [McNeal, 1976]. Between 300μA and 900μA the amplitude of P2 increased, but the amplitude of P1 did not. This resulted from activation of the small nerve fibers innervating SO. The plateaus in the curves between 600 μA and 800 μA show that the fibers innervating LG and SO were fully activated before the stimulation spread to another fascicle. Above 900μA, the amplitude of P1 increases while the amplitude of P2 remains roughly constant. The increase in P1 indicates that the large nerve fibers innervating the rapidly contracting muscle fibers of the agonist, MG, were recruited. This pattern of spillover was consistent with the neighboring location of the LG/SO and MG fascicles in the sciatic nerve. The recruitment curves for the MG and CP fascicles are shown in figures 4b and 4c. Note that the small nerve fibers innervating the muscle fibers producing P2 had a higher stimulus threshold than do the large nerve fibers innervating the muscle fibers producing P1, and that the P2 amplitudes are much smaller for the MG and the CP than for LG/SO.

Figure 5 shows a 2-dimensional vector plot of the recruitment data from figure 4. Only plantar-flexion/dorsi-flexion and toe-in/toe-out torques were plotted because

inversion/eversion torques were extremely small (< 2 N-cm at full recruitment). Note that the axis scales differ by a factor of ten, and thus the torques produced were almost entirely in the sagittal plane. The vector plots allowed determination of the direction of torques generated by both the rapidly contracting (P1) and slowly contracting (P2) motor units. The P1 and P2 vectors produced by activation of the LG/SO fascicle differed in their magnitudes and directions. The P1 vector, representative of activation of LG had a larger toe-out component than the P2 vector, which was representative of SO activation. The angle of the P1 vector (84.9°±1.6°, mean±standard deviation) was significantly less than the angle of the P2 vector (87.7°±3.0°) (n=9, p=0.0225, unpaired, 2-tailed t-test, reject null hypothesis that the angles were the same) indicating that the LG generated significantly more toe-out torque than the SO. The P1 and P2 vectors generated by activation of the MG fascicle also had different magnitudes and directions. The angle of the P1 vector (96.5°±4.4°) was significantly different than the angle of the P2 vector (107.5°±3.9°) (n=8, p=0.0001, unpaired, 2-tailed t-test, reject null hypothesis that the angles were the same). As with the MG, the P1 and P2 vectors generated by activation of CP had different directions. The angle of the P1 vector (-96.8°±8.4°) was less than the angle of the P2 vector (-106.8°±17.3°), however, the difference was not significant (n=13, p=0.0727, unpaired, 2-tailed t-test, accept null hypothesis that the angles were the same). These data indicate that the slow twitch muscle fibers within these muscles generated torques in a different direction than the torques generated by the fast twitch muscle fibers. However, the toe-in/toe-out component of P2 vectors were quite small (-1.0±0.5 N-cm for MG, -0.3±0.4 for CP), and thus the difference in direction between fast and slow muscle fibers may be an artifact due to sensor resolution.

Quantification of Activation

We hypothesized that the activation of slow twitch muscle fibers would not be represented in the peak of the twitch torque, and therefore that the peak torque would underestimate the level of activation, as compared to the torque-time integral (i.e., area under the twitch). We compared the levels of activation predicted by each measure by determining the linear correlation between the peak twitch torque and the torque-time integral for a total of 36 different recruitment curves collected in three cats (figure 6a). There was a high correlation between the two measures of activation within each animal (r^2>0.9, p=0.0001), and also when all three data sets were combined (r^2=0.942, p=0.0001). Furthermore the slope of the regression line was very similar among the three animals (14.1, 14.3, 14.9) indicating a consistent relationship between the torque time integral and the peak of the twitch torque. Thus, the peak torque proved to be a reliable summary indicator of the level of activation.

In cases where mixed fiber populations were activated (e.g., the branch of the sciatic nerve innervating the lateral gastrocnemius, predominantly fast twitch, and the soleus, exclusively slow twitch) a more complex waveshape was observed (figure 3a). In these mixed fiber responses, the peak torque and the torque-time integral were still highly correlated (r^2>0.9, p=0.0001). The correlation between the peak torque and the torque time integral did decrease when activation spread to antagonist muscles. Co-contraction of antagonists produced torque twitches with complex, polyphasic shapes (figure 6b). The effect of the spillover on the shape of the waveform varied according to the relative speed of the muscle fibers being activated. The linear correlation coefficient (r^2) decreased 12%±7% (mean±standard deviation, n=3 cases of co-contraction of antagonists) when the spillover waveforms were included in the regression analysis.

Angle Dependence of Torque Generation

Angle-dependence of torque generation appeared as differences in the scaling and shape of the recruitment curves measured at different ankle joint angles. Recruitment curves were measured at a neutral ankle angle (90°) as well as at dorsi- and plantar-flexed angles of the ankle (±20°). An example of three recruitment curves is shown in figure 7. Note that the torque output of the muscles changed as the ankle angle, and thus the muscle length, changed. As expected from the length-tension properties of muscle, the force output increased as the muscles were stretched and decreased as the muscles were shortened [Rack and Westbury, 1969]. To quantify the degree of angle-dependent recruitment (i.e., changes in output not resulting from length-tension properties or angle-dependent moment arms), torques measured at ankle angles of 110° and 70° were normalized to their maximum values and plotted as a function of the normalized torque measured at an ankle angle of 90°. The normalization process eliminates the scaling components due to the length-tension properties of muscle and the angle-dependent moment arms [Crago et al., 1980]. If there is no angle-dependence to recruitment, all points will fall on a unity slope line through the origin. In this case the magnitude of the error ranged from 0.6% to 32% of the maximum torque with a mean error of 9% and there was no correlation (r^2=0.02) between the magnitude of the error and the magnitude of the torque. This example demonstrates the ability to measure and quantify the degree of angle-dependent recruitment using this method.

DISCUSSION

A method was developed to quantify the recruitment properties of neural stimulating electrodes. An apparatus was designed and assembled to measure the three-dimensional isometric torque generated at the cat ankle joint by stimulation of the sciatic nerve. Measuring joint torque overcomes the problems of measuring isolated muscle force. Measuring torques in three dimensions provides a way to assess the net

motor output generated by specific stimulus parameters, rather than sampling activation in a discrete subset of muscles. Furthermore, isolated muscle force does not provide a clear picture of how the measured forces will translate into limb movement where muscle moment arms, distributed tendinous insertions, and muscle fiber pennation each play a role [Zajac, 1989]. Isometric ankle joint torque, however, is directly proportional to the acceleration of a limb segment upon release (a=F/m), and it has been demonstrated that isometric torques accurately predict the trajectory of limb movement upon release [Giszter et al., 1993]. Finally, this method can readily be extended to clinical application on human subjects.

The comparison of activation measures indicated that the peak of the twitch waveform is an accurate summary indicator of excitation, even in the presence of slowly contracting muscle fibers. The torque twitches, however, provided useful information about the relative speed of contraction of the activated muscle fibers, and thus the relative diameters of the innervating axons. This information is important when determining the recruitment properties of stimulating electrodes since, in general, extracellular stimulation recruits large nerve fibers at lower current amplitudes than small nerve fibers. The information in the twitch waveform is useful to study the efficacy of paradigms that have been developed to achieve natural recruitment order (i.e., activation of small nerve fibers without activation of large nerve fibers) with extracellular stimuli using either novel stimulus waveforms [Fang and Mortimer, 1990, Grill and Mortimer, 1993] or electrode geometries [Rutten et al., 1990].

The utility of the methods was demonstrated by measuring the recruitment properties of a multiple contact nerve cuff electrode. These methods can be used to quantify the recruitment properties of other neural stimulating electrodes, and have been used to study the properties of another type of cuff electrode under development in our laboratory [Tyler and Durand, 1993]. The methods described are also useful for studies of motor system physiology. The apparatus can be used to determine the torque

contributions of groups of muscles, individual muscles, or muscle sub-units [Bonsera et al., 1992, Lawrence et al., 1993]. Based on the differentiation between units of different contraction speed, the method can also be used to study the torque contributions of fast and slow motor units. Furthermore, the apparatus is useful for measuring the torque profiles produced by stimulation of "convergent force fields" in the spinal cord [Giszter et al., 1993].

ACKNOWLEDGMENTS

The authors thank Mr. Michael Miller for software development and Mr. Dustin Tyler for assistance during these experiments.

This work was supported by a grant from the Paralyzed Veterans of America Spinal Cord Research Foundation and by NIH-NINDS Neural Prosthesis Program Contract # NO1-NS-32300.

FIGURE LEGENDS

Figure 1: Apparatus to measure three-dimensional isometric torque at the cat ankle joint.

Figure 2: Definition of axes in measurement system coordinates and torque components at the cat ankle joint.

Figure 3: Examples of twitch torque waveforms recorded by selective activation of the sciatic nerve with a cuff electrode or supramaximal stimulation of individual nerve branches. Each trace shows the average plantar-flexion or dorsi-flexion torque evoked by five stimuli at the current amplitude shown above each trace. A. Twitch torque waveforms resulting from activation of the fascicle innervating the lateral gastrocnemius and the soleus. Note the large contribution of the slow twitch muscle fibers in the SO (P2). B. Twitch torque waveform resulting from activation of the fascicle innervating the medial gastrocnemius. C. Twitch torque waveform resulting from activation of the common peroneal fascicle innervating the ankle dorsi-flexors.

Figure 4: Recruitment curves of the plantar-flexion/dorsi-flexion torque contributions of the rapidly contracting muscle fibers (P1) and the slowly contracting muscle fibers (P2) as a function of the stimulus current amplitude. A. Recruitment of LG and SO. Above 900 μA ,activation spreads to MG. B. Recruitment of MG. C. Recruitment of CP fascicle.

Figure 5: Torque vectors generated by the rapidly contracting (P1) and slowly contracting (P2) muscle fibers produced by activation of each of the three components of the sciatic nerve as in figure 4.

Figure 6: A. Peak torque as a function of the torque-time integral for 36 recruitment curves in 3 cats. The peak of the torque twitch was highly correlated with the value of the torque time integral indicating that the peak torque is an accurate summary indicator of excitation. B. Examples of complex plantar-flexion/dorsi-flexion twitches generated when activation spread to antagonist muscles (compare to figure 3).

Figure 7: An example of angle dependence of torque generated by stimulation with a cuff electrode. A. Plantar-flexion torque as a function of stimulus current amplitude at three different ankle joint angles. B. Normalized plantar-flexion torque at ±20° as a function of the normalized torque at 90°. Deviations from the unity slope lines indicate angle dependence of torque generation.

REFERENCES

Ashton-Miller, J.A., Y. He, V.A. Kadhiresan, D A. McCubbrey, J.A. Faulkner (1992) An apparatus to measure in vivo biomechanical behavior of dorsi- and plantarflexors of mouse ankle. J. Appl. Physiol. 72:1205-1211.

Bonsera, S.J., J.H. Lawrence, III, and T.R. Nichols (1992) Selective recruitment within the triceps surae of the decerebrate cat alters the direction of ankle torque profiles. Soc. Neurosci. Abs. 18:149.

Bowman, B.R., and R.C. Erickson (1985) Acute and chronic implantation of coiled wire intraneural electrodes during cyclical electrical stimulation. Ann. Biomed. Eng. 13:75-93.

Burke, R.E., D.N. Levine, P. Tsairis and F.E. Zajac III (1973) Physiological types and histochemical profiles in motor units of the cat gastrocnemius. J. Physiol. 234:723-748.

Burke, R.E., D.N. Levine, M. Salcman, and P. Tsairis (1974) Motor units in cat soleus muscle: physiological, histochemical and morphological characteristics. J. Physiol. 238:503-514.

Crago, P.E., P.H. Peckham, and G.B. Thrope (1980) Modulation of muscle force by recruitment during intramuscular stimulation. IEEE Trans. Biomed. Eng. 27:679-684.

Dum, R.P, and T.T. Kennedy (1980) Physiological and histochemical characteristics of motor units in cat tibialis anterior and extensor digitorum longus muscles. J. Neurophysiology 43:1615-1630.

Fang, Z.P., and J.T. Mortimer (1992) Selective activation of small motor axons by quasitrapezoidal current pulses. IEEE Trans. Biomed. Eng. 38:168-174.

Giszter, S.F., F.A. Mussa-Ivaldi, and E. Bizzi (1993) Convergent force fields organized in the frog's spinal cord. J. Neuroscience 13:467-491.

Gorman, P.H., J.T. Mortimer (1983) The effect of stimulus parameters of the recruitment characteristics of direct nerve stimulation. IEEE Trans. Biomed. Eng. 30:407-414.

Gorman, P.H., P.H. Peckham (1991) Upper extremity functional neuromuscular stimulation. J. Neuro. Rehab. 5:3-11.

Grandjean, P.A., and J.T. Mortimer (1986) Recruitment properties of monopolar and bipolar epimysial electrodes. Ann. Biomed. Eng. 14:53-66.

Grill, W.M. and J.T. Mortimer (1993) Selective activation of distant nerve fibers. Proc. 15th Int. Conf. IEEE Eng. Med. Biol. Soc. 15(3):1328-1329.

Hoffer, J.A. (1990) Techniques to study spinal-cord, peripheral nerve, and muscle activity in freely moving animals. in A.A. Boulton, G.B. Baker, and C.H. Vanderwolf (Eds.), Neuromethods, Vol. 15: Neurophysiological Techniques: Applications to Neural Systems. The Humana Press Inc., Clifton, N.J., pp. 65-145.

Lawrence, J.H., III, T.R. Nichols, and A.W. English (1993) Cat hindlimb muscles exert substantial torques outside the sagittal plane. J. Neurophys. 69:282-285.

Marsolais, E.B., and R. Kobetic (1987) Functional electrical stimulation for walking in paraplegia J. Bone and Joint Surg. 69-A:728-733.

McNeal, D.R. (1976) Analysis of a model for excitation of myelintated nerve. IEEE Trans. Biomed. Eng. 23:329-338.

McNeal, D.R., L.L. Baker, and J.T. Symons (1989) Recruitment data for nerve cuff electrodes: implications for design of implantable stimulators. IEEE Trans. Biomed. Eng. 36:301-308.

McNeal, D.R., and B.R. Bowman (1985) Selective activation of muscles using peripheral nerve electrodes. Med. and Biol. Eng. and Comp, 23:249-253.

Memberg, W.D., P.H. Peckham, G.B. Titrope, M.W. Keith, T.P. Kicher (1993) An analysis of the reliability of percutaneous intramuscular electrodes in upper extremity FNS applications. IEEE Trans. Rehab. Eng. 1:126-132.

Mortimer, J.T., and W.M. Grill (1993) Cuff electrodes for motor prostheses. Proc. Ljubljana FES Conference, Ljubljana, Slovenia, 15-18.

Nannini, N., and K. Horch (1991) Muscle recruitment with intrafascicular electrodes. IEEE Trans. Biomed. Eng. 38:769-776.

Naples, G. G., J. T. Mortimer, and T.G.H. Yuen (1990) Overview of peripheral nerve electrode design and implantation. in W.F. Agnew and D.B. McCreery, Eds., Neural Prostheses: Fundamental Studies, Prentice Hall, Englewood Cliffs, New Jersey, pp. 107-145.

Rack, P.M.H., and D.R. Westbury (1969) The effects of length and stimulus rate on tension in the isometric cat soleus muscle. J. Physiol. 204:443-460.

Rutten, W.L.C., H.J. van Wier, and J.H.M. Put (1991) Sensitivity and selectivity of intraneural stimulation using a silicon electrode array. IEEE Trans. Biomed. Eng. 38:192-198.

Stein, R.B., P.H. Peckham, D.B. Popovic (1992) Neural Prostheses: Replacing motor function after disease or disability. Oxford University Press, New York.

Thoma, H., H. Gerner, J. Holle, P. Kluger, W. Mayr, B. Meister, G. Schwanda, H. Stohr (1987) The phrenic pacemaker: substitution of paralyzed functions in tetraplegia. Am. Soc. Artif. Int. Organs Trans. 10:472-479.

Tyler, D.J., and D. Durand (1993) Design and acute test of a radially penetrating interfascicular nerve electrode. Proc. 15th Int. Conf. IEEE Eng. Med. Biol. Soc. 15(3):1247-1248.

Veraart C., W.M. Grill, and J.T. Mortimer (1993) Selective control of muscle activation with a multipolar nerve cuff electrode. IEEE Trans. Biomed. Eng. 40:640-653.

Young, R.P., S.H. Scott, and G.E. Loeb (1992) An intrinsic mechanism to stabilize posture: joint-angle-dependent moment arms of the feline ankle muscles. Neur. Letters 145:137-140.

Zajac, F.E. (1989) Muscle and tendon: properties, models, scaling, and application to biomechanics and motor control. CRC Crit. Rev. Biomed. Eng. 17:359-411.

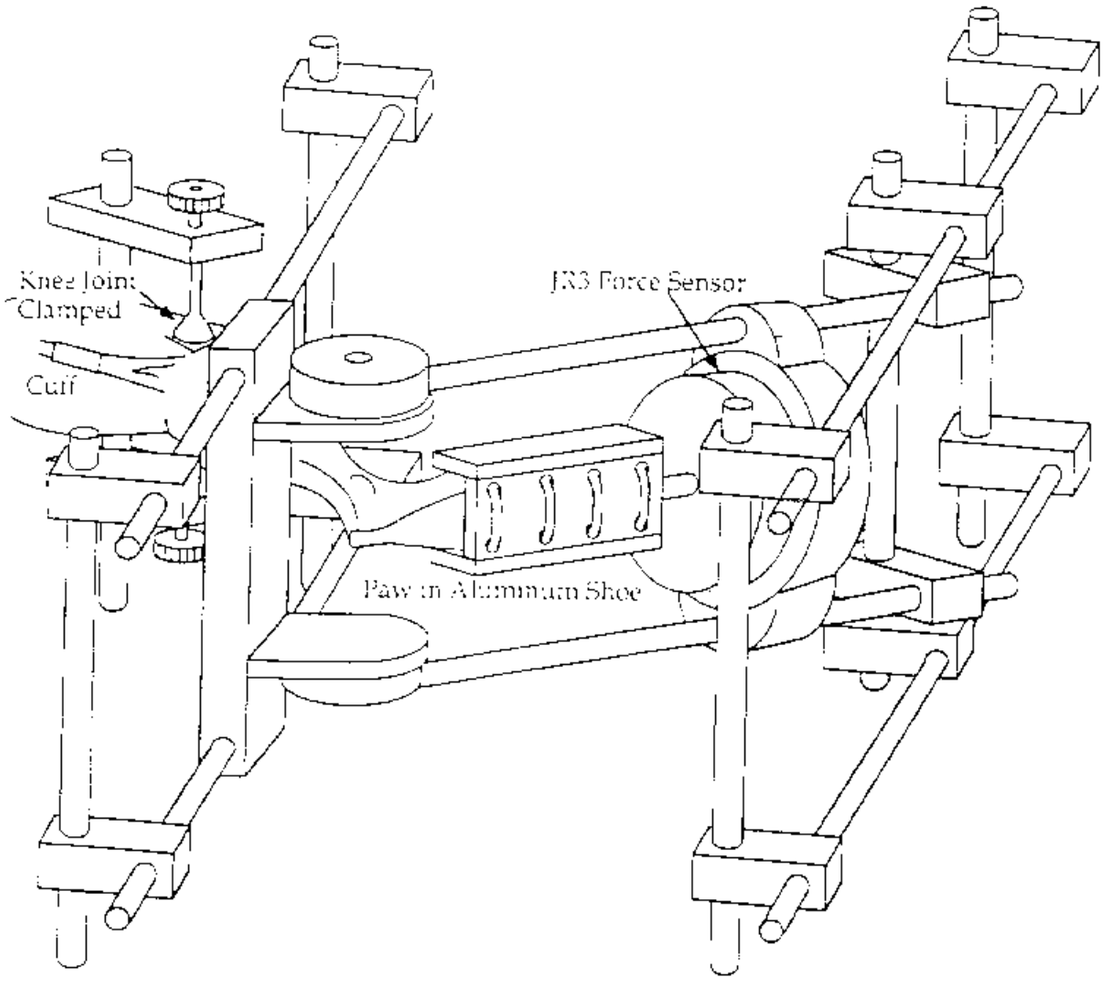
Knee Joint
Clamped
Cuff
JR3 Force Sensor
Paw in Aluminum Shoe

Figure 1

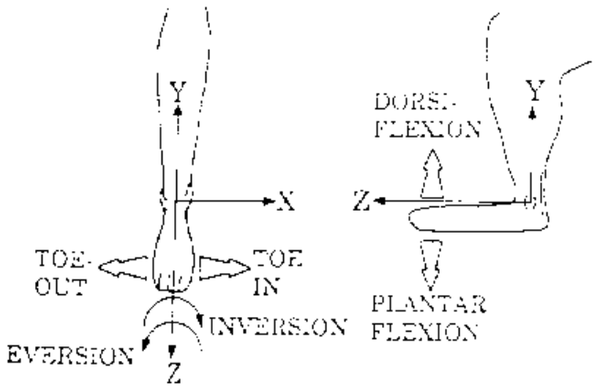
Y
X
Z
TOE-
OUT
TOE
IN
INVERSION
EVERSION
Z
DORSI-
FLEXION
Y
PLANTAR
FLEXION

FIGURE 2

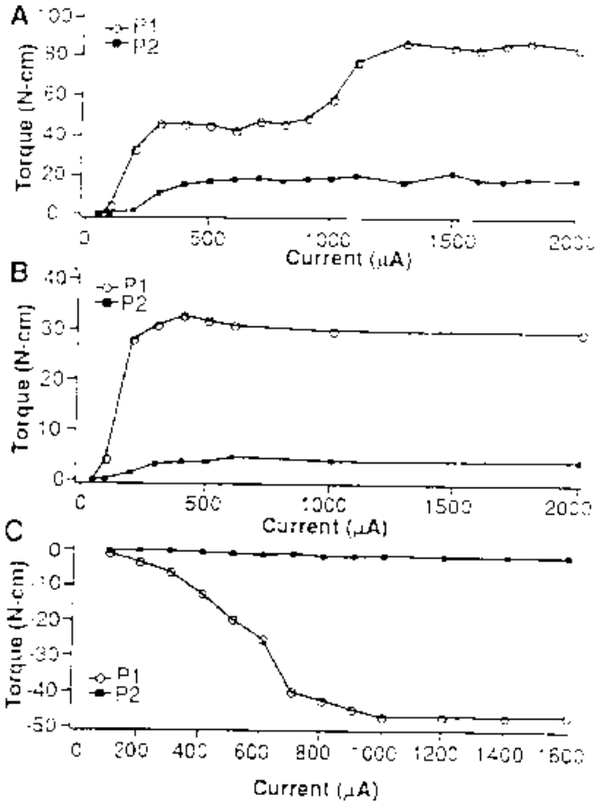
A
P1
P2
Torque (N-cm)
Current (μA)
B
P1
P2
Torque (N-cm)
Current (μA)
C
P1
P2
Torque (N-cm)
Current (μA)

Figure 4

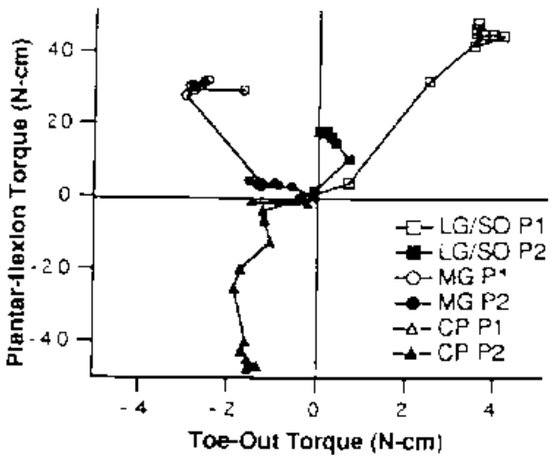
Plantar-flexion Torque (N-cm)
40
20
0
-20
-40
-4
-2
0
2
4
Toe-Out Torque (N-cm)
LG/SO P1
LG/SO P2
MG P1
MG P2
CP P1
CP P2

Figure 5

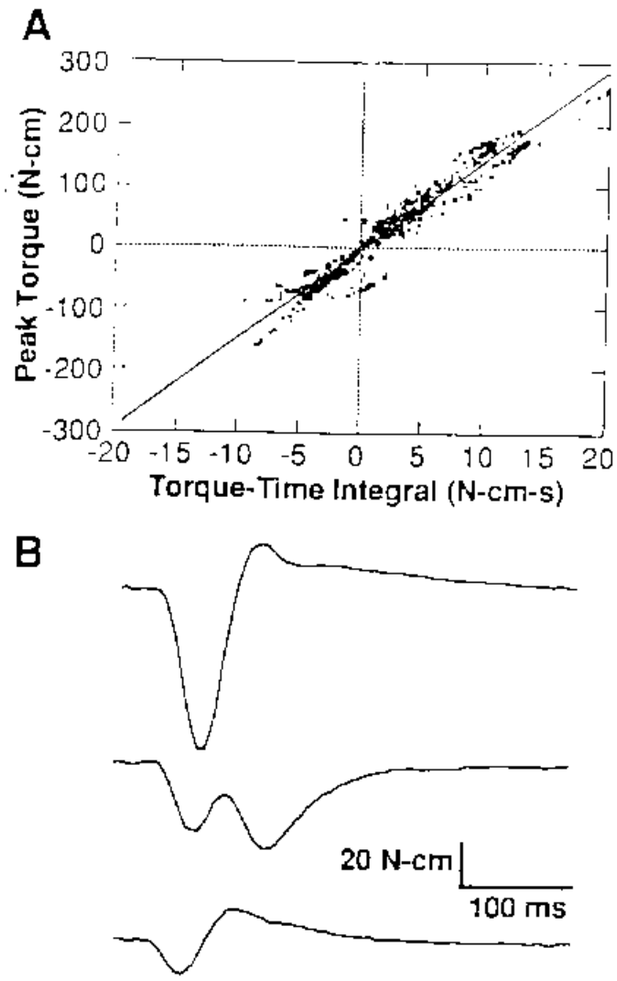
A
300
200
100
0
-100
-200
-300
Peak Torque (N-cm)
-20 -15 -10 -5 0 5 10 15 20
Torque-Time Integral (N-cm-s)
B
20 N-cm
100 ms

Figure 6

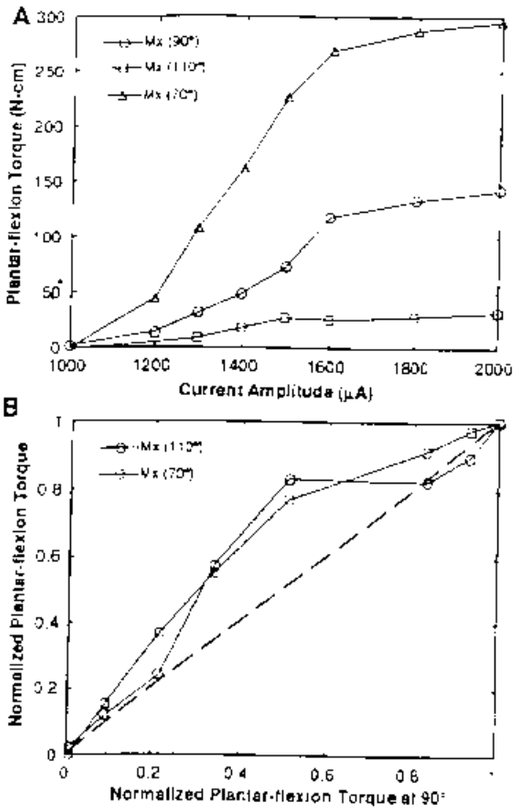
A
Mx (90°)
Mx (110°)
Mx (70°)
Plantar-flexion Torque (N-cm)
300
250
200
150
100
50
0
1000
1200
1400
1600
1800
2000
Current Amplitude (μA)
B
Mx (110°)
Mx (70°)
Normalized Plantar-flexion Torque
1
0.8
0.6
0.4
0.2
0
0
0.2
0.4
0.6
0.8
Normalized Plantar-flexion Torque at 90°

Figure 7